Available online at www.sciencedirect.com
ScienceDirect
Electrochimica Acta 52 (2006) 1491–1498
ELECTROCHIMICA Acta
www.elsevier.com/locate/electacta

Effects of metal source in metal substitution of lithium manganese oxide spinel

Ali Eftekhari *, Abdolmajid Bayandori Moghaddam, Bahareh Yazdani, Fathollah Moztarzadeh

Laboratory of Electrochemistry, Materials and Energy Research Center, P.O. Box, 14155-4777, Tehran, Iran

Received 19 October 2005; received in revised form 3 February 2006; accepted 24 February 2006
Available online 15 May 2006

Abstract

Usefulness of W substitution for improvement of battery performance of $LiMn_2O_4$ cathode was investigated. Small amounts of tungsten were incorporated into $LiMn_2O_4$ spinel instead of available Mn. For this purpose, two sources of tungsten (metallic W or WO_3) were examined. W concentration and source have significant influence on both morphology and electrochemical behavior of W-substituted $LiMn_2O_4$ spinels. W substitution of $LiMn_2O_4$ spinel can lead to the formation of uniform spinel particles and improved battery performance. Cyclic voltammetric behaviors of the samples were examined in an aqueous solution, and Li diffusion process was investigated for different cases. The best case was the $LiW_{0.01}Mn_{1.99}O_4$ spinel prepared from metallic W powder, as exhibits excellent rate capability, but better cycleability was observed for the $LiW_{0.01}Mn_{1.99}O_4$ spinel prepared from WO_3. This means that because of significant influence of the dopant source, this parameter should be chosen in respect with the desire improvement.

Keywords: Lithium battery; Cathode material; $LiMn_2O_4$; Metal substitution; Material morphology; W dopant

1. Introduction

Valuable advantages of $LiMn_2O_4$ as a potential candidate for cathodes of lithium batteries are well-known. However, further advancement is needed to overcome common problems of this cathode material. One of the most efficient approaches in this context is metal substitution of Mn in $LiMn_2O_4$ spinel [1–7]. This can reduce the amount of Mn^{3+}, which is the general goal of Mn substitution, and strengthen the structural stability of the spinel. As it has been found that metal substitution of $LiMn_2O_4$ can lead to the appearance of 5 V redox systems [8–15], this approach has recently reached a considerable attention.

Various transition metals have been employed for this purpose, but less attention had been paid to tungsten, though it is a common transition metal in electrochemical systems. This failure can be attributed to apparent disadvantage of this action, as oxidation state of W is higher than Mn and metal substitution may reduce Mn valence which is unfavorable. However, recent report of Chitrakar et al. [16] regarding usefulness of substitution of Mn in $LiMn_2O_4$ by pentavalent antimony provides a new opportunity. On the other hand, it will be discussed that the problem of reduction of Mn valence is not important for the case of W substitution (as the amount of dopant is low). In the present study, we would like to examine usefulness of W substitution for improvement of electrochemical performance of $LiMn_2O_4$. As we have emphasized before, it is more appropriate to investigate preliminary electrochemical studies of new cathode materials in aqueous media rather than non-aqueous media [17,18]. In fact, aqueous electrolytes contain simple components and the exact electrochemical performance of cathode material can be detected. Whereas, additional process can be occurred in non-aqueous electrolytes, leading to different electrochemical performances. For instance, a considerable attention has been paid to the instability of electrolytes in lithium batteries [19–21]. Thus, it cannot be concluded that the improvements observed are due to better cathode material or better electrolyte stability on the electrode surface. On the other hand, aqueous media are also potential candidates to replace conventional non-aqueous media of lithium batteries and considerable attention has been recently paid to them [22–25].

* Corresponding author. Tel.: +98 261 621 0009; fax: +98 261 620 1888..
E-mail address: eftekhari@merc.ac.ir (A. Eftekhari).

0013-4686/$ – see front matter © 2006 Elsevier Ltd. All rights reserved.
doi:10.1016/j.electacta.2006.02.049

2. Experimental

Cathode materials were synthesized by conventional solid-state reaction. Stoichiometric amounts of raw materials were completely mixed by ball milling. Appropriate amounts of tungsten were added from the sources of tungsten oxide or metallic W fine powder. For solid-state synthesis, the furnace temperature was slowly increased with the rate of 1 °C/min to reach the temperature of 800 °C. Slow heating provides an appropriate opportunity for preliminary decomposition of raw materials such as carbonates. The temperature was fixed at 800 °C for 40 h and then the furnace was slowly cooled to room temperature. The composite electrodes for electrochemical studies were prepared from mixture of active material and acetylene black in the ratio of 1:1. For casting the composite, a drop of melted paraffin was added.

Cyclic voltammetric studies were performed using a Metrohm 746 VA potentiostat.

Electrolyte was aqueous solution of saturated lithium nitrate. Potentiostatic experiments were performed using a Princeton Applied Research potentiostat/galvanostat model 173 (PAR 173) equipped with a model 175 universal programmer in conjunction with CorrView software. In the experimental measurements, all potentials were referenced to a saturated calomel electrode (SCE), but the potentials were calculated in reference to conventional Li/Li^+. Scanning electron microscopic (SEM) investigations were carried out using a Cambridge scanning electron microscope model Steroscan 360. Powder Xray diffractions (XRD) were recorded using a Phillips PW 1371 diffractometer based on Cu Kα radiation.

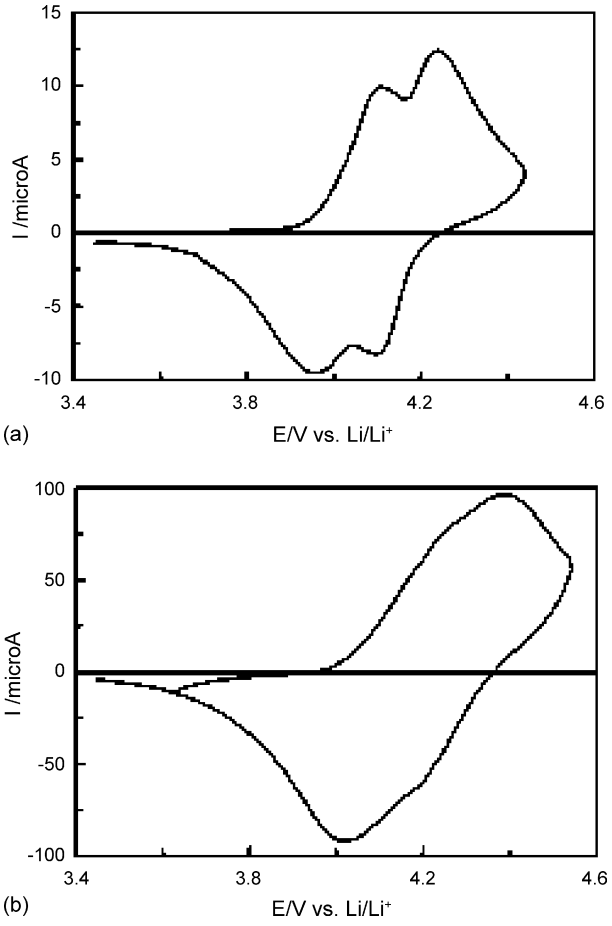

Fig. 1. Typical cyclic voltammograms of $LiMn_2O_4$ spinels synthesized from raw materials of (a) Li_2CO_3, and (b) LiOH. Electrolyte was a saturated solution of $LiNO_3$ and scan rate 0.5 mV/s.

3. Results and discussion

It is known that the source of lithium in solid-state synthesis has a significant influence on the battery performance of $LiMn_2O_4$ spinel [26], as lithium should be extracted and inserted from/into the spinel structure in the course of cycling. The best case is lithium carbonate, which decomposes at smaller temperatures before the occurrence of the main solid-state reaction. Of course, this also depends on manganese raw material, which for the present study was $MnCO_3$. Another alternative is lithium hydroxide, but as its decomposition is not as well as lithium carbonate, $LiMn_2O_4$ spinel prepared from LiOH has not well-defined electrochemical behavior as well as that prepared from Li_2CO_3 (Fig. 1). Of course, this does not mean that $LiMn_2O_4$ prepared from LiOH is not applicable for battery performance. Note that the cyclic voltammetric behaviors presented in Fig. 1 are related to a relatively fast scan (for the case of lithium batteries), and the $LiMn_2O_4$ prepared from LiOH displays a well-defined behavior at slower scans. In fact, we use this critical condition to inspect the difference of two cases. Of course, this is a tricky reason, but the main reason for this choice is that LiOH is a cheaper source for synthesis of $LiMn_2O_4$. In other words, it is of commercial interest to improve synthesis of $LiMn_2O_4$ from LiOH because of cost reason.

In other words, these studies reveal rate capability of the cathode materials, similar to conventional galvanostatic studies of battery performance of cathode materials at different C rates [24,27–29]. Here, we aim to inspect the rate capabilities of the W-substituted $LiMn_2O_4$ cathode materials using cyclic voltammetric studies in aqueous media (this issue will be described further). We will continue this strategy to inspect the influence of W substation on electrochemical behavior of $LiMn_2O_4$. In other words, the W-substituted $LiMn_2O_4$ spinels were synthesized from LiOH and their electrochemical behaviors should be compared with Fig. 1b (of course, W-substituted $LiMn_2O_4$ spinels were also synthesized from Li_2CO_3, but the results were not distinguishable like the present case).

Not only the source of lithium raw material, but also the source of substituting metal has a significant influence on the material properties of $LiMn_2O_4$ spinel. The sources of substituting metals are usually their oxides. However, when the dopant concentration is low (e.g. the case of noble metal substitution), it is possible to use metallic powders [30]. At the condition of high-temperature solid-state synthesis under air atmosphere, the metallic powders will be completely oxidized, and no significant difference is expected. Since the amount of W in $LiMn_2O_4$ is small, we will examine two afore-mentioned sources of tungsten for metal substitution of $LiMn_2O_4$. The results will be reported separately and compared later.

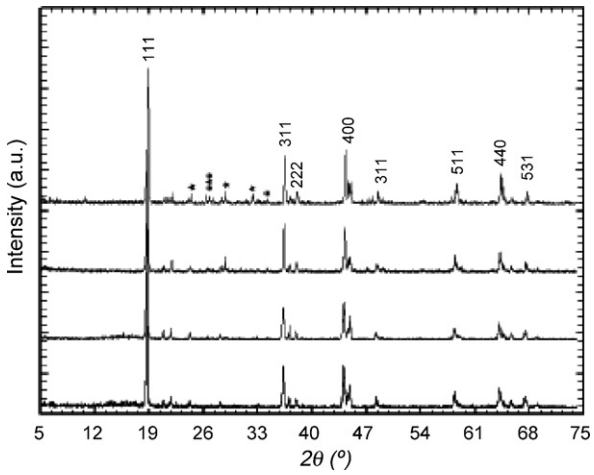

Fig. 2. XRD patterns of W-substituted $LiMn_2O_4$ spinels prepared from raw material of metallic W powder, as the amounts of W in $LiW_xMn_{2-x}O_4$ were (a) $x=0$, (b) $x=0.01$, (c) $x=0.05$, and (d) $x=0.1$. (a)–(d) patterns are from bottom to top, respectively. The impurity peaks corresponding to unsuccessful doping of W are indicated by asterisks.

Fig. 2 presents XRD patterns of W-substituted $LiMn_2O_4$ spinels with different W concentrations. As expected such small amounts of substituting metal do not affect the spinel structure, and even for the highest concentration a well-defined structure of cubic spinel with space group of *Fd3m* which is related to structure of $LiMn_2O_4$ is detectable. Of course, there are some impurity peaks, independent of the W added (even for the virgin $LiMn_2O_4$) in addition to original peaks of $LiMn_2O_4$ spinel. These impurity peaks which constantly exist for all cases are due to low crystallinity of $LiMn_2O_4$ spinel prepared from Li source of LiOH. This is indeed a failure of LiOH in comparison with Li_2CO_3 which is easily decomposed to generate pure $LiMn_2O_4$ spinel. In any case, some tiny peaks are appeared as a result of W doping. These are indeed impurity peaks appearing for higher amounts of W dopant. The place of impurity peaks indicated in the XRD patterns can be indexed to common W oxides. For instance, three close impurity peaks indicated in Fig. 2d recalls three characteristic peaks of WO_3 with space group of P21/n (JCPDS 43-1035). In other words, W doping is restricted by a limit of ca. 0.01 in $LiW_xMn_{2-x}O_4$. Comparison of two XRD patterns corresponding to virgin $LiMn_2O_4$ and $LiW_{0.01}Mn_{1.99}O_4$ spinels by means of Rietveld refinement indicates that W (at least in low amounts) has occupied the Mn sites. This conclusion cannot be made for the spinels prepared by higher amounts of dopant due to poor fitting.

In any case, substitution slightly decreases the spinel lattice constant. Since the general structure is cubic spinel for all cases, it is useful to compare lattice structure of the spinels synthesized to inspect the role of W dopant. This decrease is stronger for higher W concentrations (Table 1). Although, the ionic radius of W is higher than that of Mn, this behavior is ordinary as it was also observed for other heavy transition metals [17,31]. The reason for this behavior is stronger (and subsequently shorter) bonds of such metals with oxygen in comparison with Mn–O bond.

Table 1
Lattice constants of W-substituted $LiMn_2O_4$ spinels

Sample	Raw material	Lattice constant(Å)
$LiMn_2O_4$	N/A	8.234 ± 0.001
$LiW_{0.01}Mn_{1.99}O_4$	Metallic W	8.230 ± 0.001
$LiW_{0.05}Mn_{1.95}O_4$	Metallic W	8.224 ± 0.001
$LiW_{0.1}Mn_{1.9}O_4$	Metallic W	8.212 ± 0.001
$LiW_{0.01}Mn_{1.99}O_4$	WO_3	8.233 ± 0.001
$LiW_{0.05}Mn_{1.95}O_4$	WO_3	8.229 ± 0.001
$LiW_{0.1}Mn_{1.9}O_4$	WO_3	8.225 ± 0.001

Fig. 3 illustrates a series of SEM images of W-substituted $LiMn_2O_4$ spinels with different amounts of W. Higher atomic radius of W in comparison with Mn may induce such an idea that W can not be substituted in $LiMn_2O_4$ structure during the thermal treatment and it just coats the $LiMn_2O_4$ surface. However, paying more attention to SEM images refuses this idea because W substitution highly affected the powder morphology of $LiMn_2O_4$ spinel, and appearance of such morphological changes by thermal treatment in the absence of W substitution is unlikely. More concentrating on SEM images reveals that the conventional $LiMn_2O_4$ spinel has crystalline particles but with a large range of particle size distribution (Fig. 3a). W substitution leads to the formation of uniform particles (Fig. 3b). Among these uniform rectangular particles, some spherical particles are also formed. For higher W concentrations, the amount of such spherical particles increases and the particles uniformity disappears (Fig. 3c and d). For the $LiW_{0.1}Mn_{1.9}O_4$ sample, the conventional rectangular particles of $LiMn_2O_4$ spinel are approximately absent (Fig. 3d).

Cyclic voltammetric measurements of different $LiW_xMn_{2-x}O_4$ cathode materials (Fig. 4) indicate that W substitution may lead to better electrochemical performance, but this is highly concentration-dependent. When $x=0.01$ in $LiW_xMn_{2-x}O_4$, the electrochemical performance is improved and the rate capability is enhanced (as comparing Fig. 4a with Fig. 1b). For higher concentrations, the two characteristic peaks of $LiMn_2O_4$ are overlapped. This does not mean that actual redox system of the $LiW_xMn_{2-x}O_4$ is changed (in comparison with well-defined redox systems of $LiMn_2O_4$), but this indicates that the cathode material has not appropriate rate capability to display the well-defined redox system at this relatively high scan rate, however, the well-defined redox system can once again be detected at slower scans.

In general, all cases of W substitution improves electrochemical performance of the $LiMn_2O_4$ cathode material (note that the results should be compared with Fig. 1b, not Fig. 1a), but the case of $LiW_{0.01}Mn_{1.99}O_4$ is the best. It is worth noting that W substitution (particularly when $x=0.01$) in the case of Li_2CO_3 raw material also improves the electrochemical performance of the $LiMn_2O_4$ cathode material in comparison with Fig. 1a, but as the virgin $LiMn_2O_4$ has well-defined redox system in this case (Fig. 1a), this difference is not obviously distinguishable unless using higher scan rates as the well-defined redox of conventional $LiMn_2O_4$ begins to disappear. After investigating W substitution from metallic W powder as raw material

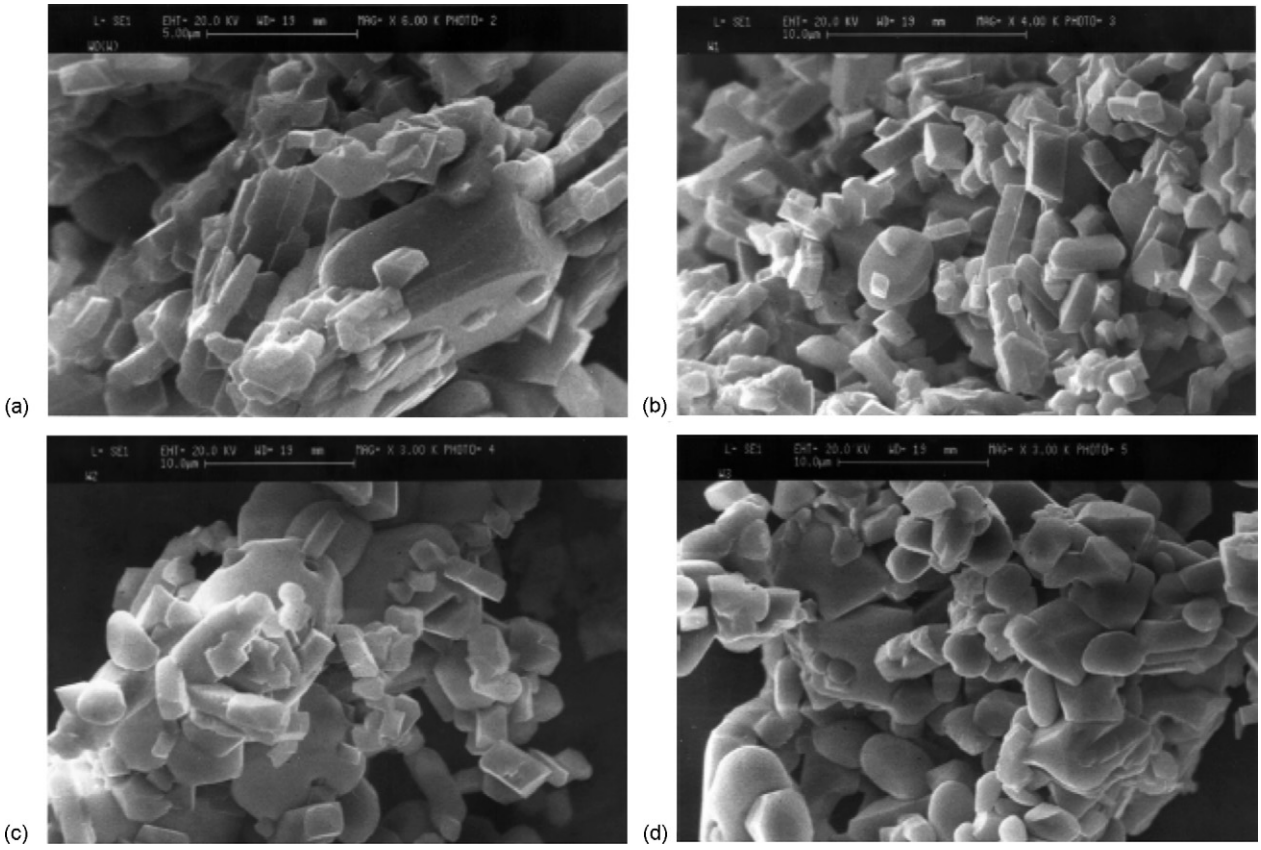

Fig. 3. SEM images of the samples (a)–(d) in Fig. 2.

(Figs. 2–4), it is appropriate to investigate W substitution from common raw material of metal oxide, i.e., WO_3. XRD patterns of $LiW_xMn_{2-x}O_4$ spinels synthesized from WO_3 are presented in Fig. 5. It is obvious that the patterns are similar to those obtained from metallic W powder as raw material, and the arguments mentioned above are completely justified here. Of course, it seems that the impurity peaks corresponding to W oxide is weaker in this case, as the three characteristic peaks of WO_3 quoted above is no longer distinguishable in Fig. 5d. In any case, there is a significant difference in the degree of decrease in the lattice constant. This is more obvious from the data summarized in Table 1. In fact, the lattice constant is less affected when WO_3 is employed as the source of W dopant. Although formation of strong W–O bonds is more likely during in situ oxidation of metallic W (Fig. 2d), the incorporation of W dopant when it is already oxidized (the source of WO_3) is easier (Fig. 5d).

Morphological changes of the $LiW_xMn_{2-x}O_4$ spinels when synthesized from WO_3 are different from those prepared from metallic W powder. As shown in Fig. 6a, for the case of $LiW_{0.01}Mn_{1.99}O_4$ synthesized from WO_3, the particles uniformity detected for the case of metallic W raw material (as illustrated in Fig. 3a) is not obvious. In this case, there is a tendency for the formation of long rod-like particles (Fig. 6a). For the case of $LiW_{0.05}Mn_{1.95}O_4$, no tendency for the formation of spherical particles is observed (Fig. 6b). Although the shape of the $LiW_{0.1}Mn_{1.9}O_4$ spinel synthesized from WO_3 is different from that prepared by metallic W raw material, the spherical shape of particles again appears (Fig. 6c).

Electrochemical behaviors of the $LiW_xMn_{2-x}O_4$ cathode materials synthesized from WO_3 raw material are similar to those prepared from metallic W raw material (as comparing Fig. 4 and Fig. 7), but not as well as those. In other words, W substitution from WO_3 also improves the rate capability of $LiMn_2O_4$ (Fig. 7) but not as much as W substitution from metallic W powder (Fig. 4).

The results reported above suggest that the best W concentration is $x = 0.01$. This means that W substitution is optimized for the case of $LiW_{0.01}Mn_{1.99}O_4$, whether using metallic W powder or WO_3 as raw materials. Of course, using metallic W powder leads to better results (Fig. 4a). Therefore, we concentrate on this optimum case (i.e. $LiW_{0.01}Mn_{1.99}O_4$ spinel) for further investigations. It seems that W substitution from metallic W raw material leads to the appearance of well-defined redox system of $LiMn_2O_4$ (Fig. 4a); whereas, using WO_3 raw material is accompanied by partial loss of the well-defined redox system as the two redox couples tend to merge together (Fig. 7a). Once again, we emphasize that this is just due to the difference of rate capabilities, not change in the origin of redox systems. Comparison of cyclic voltammograms of two different $LiW_{0.01}Mn_{1.99}O_4$ samples at a sufficiently slow scan reveals this issue (Fig. 8). The electrohemical behaviors are similar and no significant difference can be distinguished. Similar behaviors (such well-defined shape of cyclic voltammograms) can be detected for other cases

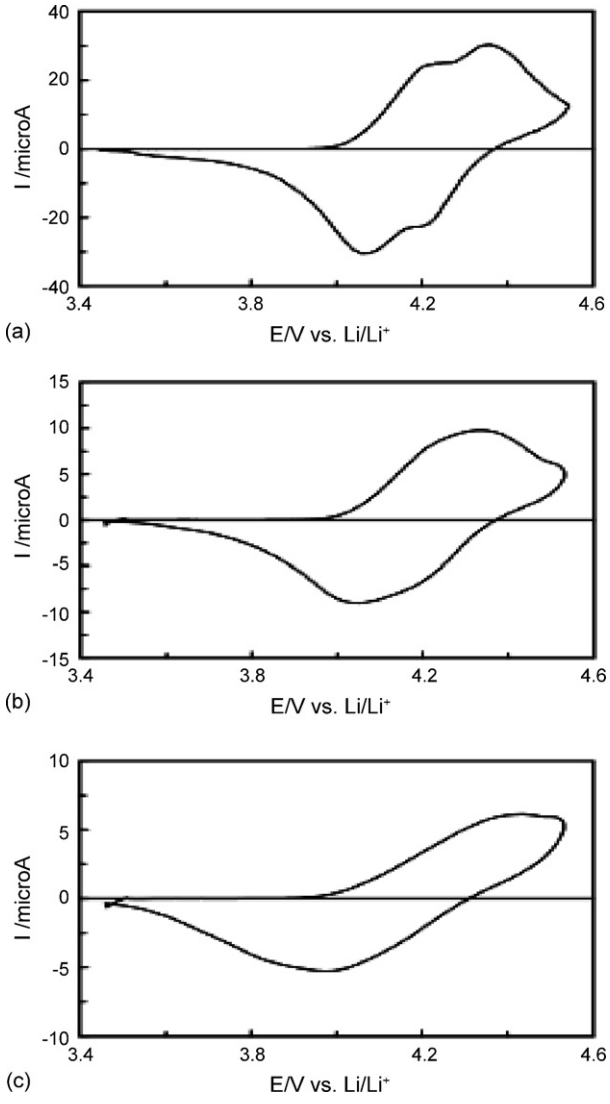

Fig. 4. Cyclic voltammetric behaviors of the W-substituted $LiMn_2O_4$ spinels prepared from raw material of metallic W powder, as the amounts of W in $LiW_xMn_{2-x}O_4$ were (a) $x = 0.01$, (b) $x = 0.05$, and (c) $x = 0.1$. The electrolyte solution was saturated lithium nitrate. Scan rate 0.5 mV/s.

(Fig. 1b, Fig. 4b,c, Fig. 7b,c) when recording cyclic voltammograms at lower scan rates. This distinguishable change of the shape of cyclic voltammograms was the reason for choosing this critical scan rate (i.e. 0.5 mV/s) for the present study.

Throughout the manuscript, we talked about the difference in rate capabilities of different W-substituted $LiMn_2O_4$ cathode materials. It is well known that rate capability is related to the diffusion of Li ion in the course of intercalation/ deintercalation process. Thus, it is appropriate to inspect the diffusion coefficient of Li ions. The diffusion coefficients were measured at different potentials by means of chronoamperometric measurements in accordance with the method described elsewhere [17]. It has been emphasized that diffusion process for such electrochemical systems is nonlinear and strongly potential dependent [32]. The general shape of the plot of diffusion coefficient versus potential for $LiMn_2O_4$ is accompanied by two minimum peaks at the potentials of the redox couples [33]. By this potentiostatic

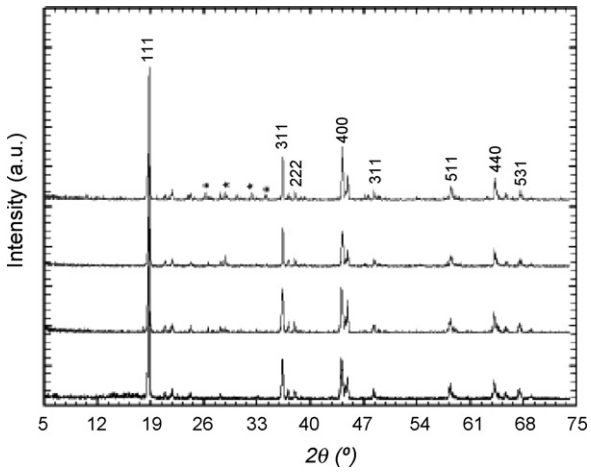

Fig. 5. XRD patterns of W-substituted $LiMn_2O_4$ spinels prepared from raw material of tungsten oxide (WO_3), as the amounts of W in $LiW_xMn_{2-x}O_4$ were (a) $x = 0$, (b) $x = 0.01$, (c) $x = 0.05$, and (d) $x = 0.1$. (a)–(d) patterns are from bottom to top, respectively. The impurity peaks corresponding to unsuccessful doping of W are indicated by asterisks.

method, it is possible to monitor the potential dependency of the diffusion coefficient even for systems involving sharp redox peaks [34].

Fig. 9 shows the diffusion coefficients estimated at various potentials for the $LiW_{0.01}Mn_{1.99}O_4$ cathode materials prepared from different raw materials. It is obvious that both of them are similar and indicate an inverse shape of the cyclic voltammograms. Similar plots were also obtained for other cases ($LiW_xMn_{2-x}O_4$ series). The important consequence of these plots is not their shapes, but the diffusion coefficient values. The diffusion coefficient for the case of $LiW_{0.01}Mn_{1.99}O_4$ cathode prepared from metallic W powder is more than one order of magnitude higher than that of original $LiMn_2O_4$. This enhancement is slightly weaker for the case of $LiW_{0.01}Mn_{1.99}O_4$ cathode material prepared from WO_3. In fact, the diffusion coefficients were proportional to the rate capabilities detected in cyclic voltammetric measurements. It should be emphasized that such differences in the diffusion coefficient are not related to the sample morphology or particle size distribution, as the experiments have been performed at sufficiently slow rate to provide required opportunity for the occurrence of solid-state diffusion. In other words, the electrochemical signal is mainly related to the diffusion process occurred inside the particles rather than on their surfaces. On the other hand, although the morphological changes of the samples are significant but this significance is in shape not in size. This argument is valid for the voltammetric studies performed under low scan rate, and also the diffusion coefficients reported in Fig. 9, as they were calculated under steady state condition by means of chronoamperometric measurements.

In addition to rate capability, the most important problem associated with $LiMn_2O_4$ spinel is poor cycleability (particularly at elevated temperatures). In fact, the main goal of metal substitution is to improve this failure of $LiMn_2O_4$ spinel. Here, we do not aim to investigate such battery performances, as falls out of the scope of the present manuscript, which aims to introduce this novel cathode material by investigating its

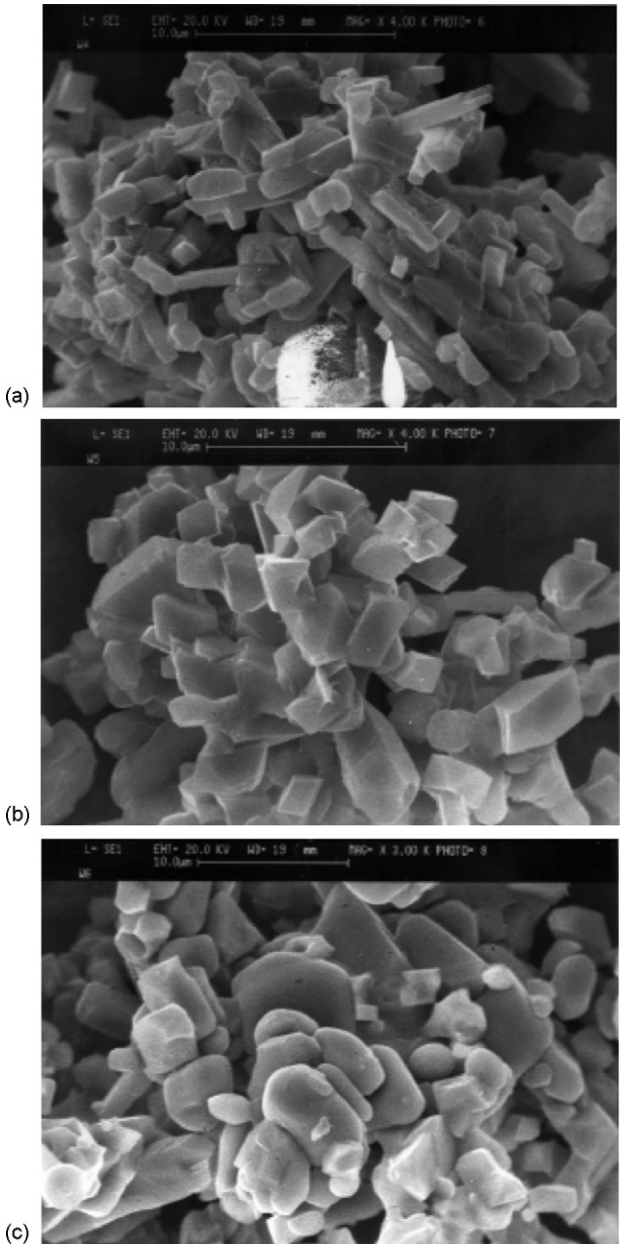

Fig. 6. SEM images of (a) $LiW_{0.01}Mn_{1.99}O_4$, (b) $LiW_{0.05}Mn_{1.95}O_4$, and (c) $LiW_{0.1}Mn_{1.9}O_4$ spinels prepared from WO_3 raw material.

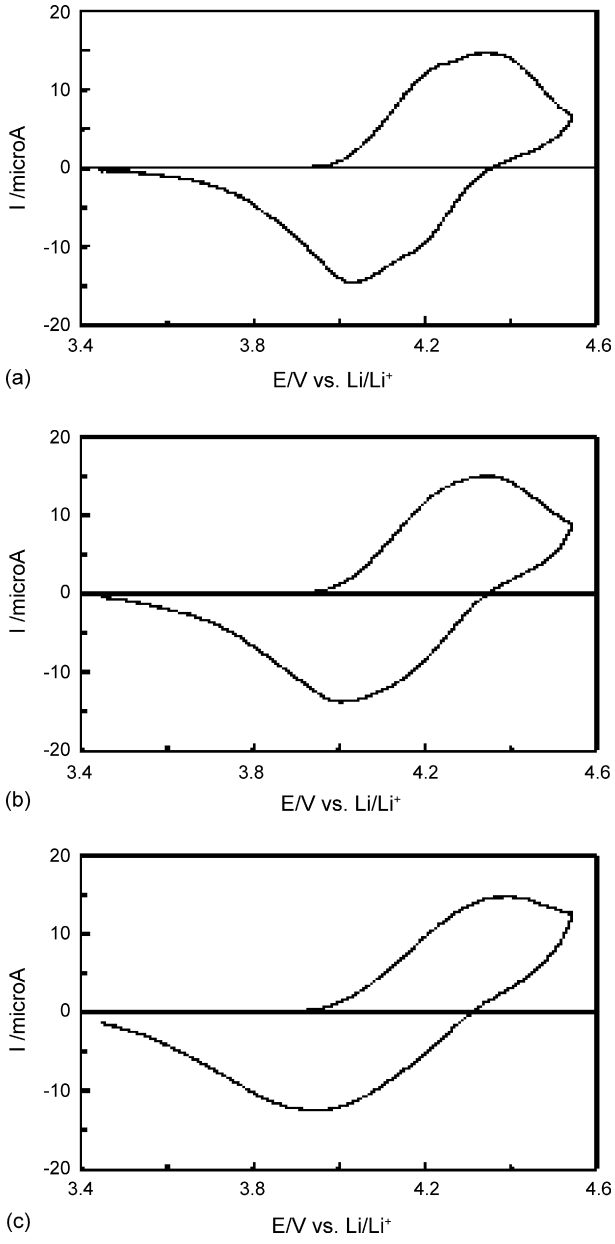

Fig. 7. Cyclic voltammograms of (a) $LiW_{0.01}Mn_{1.99}O_4$, (b) $LiW_{0.05}Mn_{1.95}O_4$, and (c) $LiW_{0.1}Mn_{1.9}O_4$ samples (prepared from WO_3 raw material) in aqueous solution of saturated $LiNO_3$. Scan rate 0.5 mV/s.

electrochemical performance. However, it is useful to compare cycleability of the W-substituted $LiMn_2O_4$ cathodes with the virgin $LiMn_2O_4$ cathode to reveal the potential usefulness of W substitution for improvement of cycleability of $LiMn_2O_4$ cathode.

Fig. 10 shows this feature. Cycleability data achieved from integrated surface of each cycle in potentiodynamic charge/discharge profiles.

It is obvious that W substitution significantly improves the cycleability of $LiMn_2O_4$ (Fig. 10). This may be attributed to the stronger W–O bond appearing in the $LiMn_2O_4$ structure, which can strengthen the spinel structure. For such a small amount of dopant ($LiW_{0.01}Mn_{1.99}O_4$), changing the Mn valence is not important. Even upon increase of the Mn valence by hexavalent W, this is not a significant disadvantage. On the other hand, decrease of Mn valance is accompanied by increase of the lattice constant [35], but inverse behavior was observed for W substitution. It is well known that cycleability of $LiMn_2O_4$ is better for smaller lattice constants [36]. In fact, decrease of lattice constant by W substitution is due to stabilized spinel structure owing to W distribution across the spinel structure forming strong W–O bonds.

However, a peculiar phenomenon still exists regarding the differences in lattice constant and consequently cycleabilities of two $LiW_{0.01}Mn_{1.99}O_4$ samples prepared from different raw materials. For the case of $LiW_{0.01}Mn_{1.99}O_4$ spinel synthesized from metallic W powder, the lattice constant is smaller than that prepared from WO_3. It seems that since oxidation of metallic

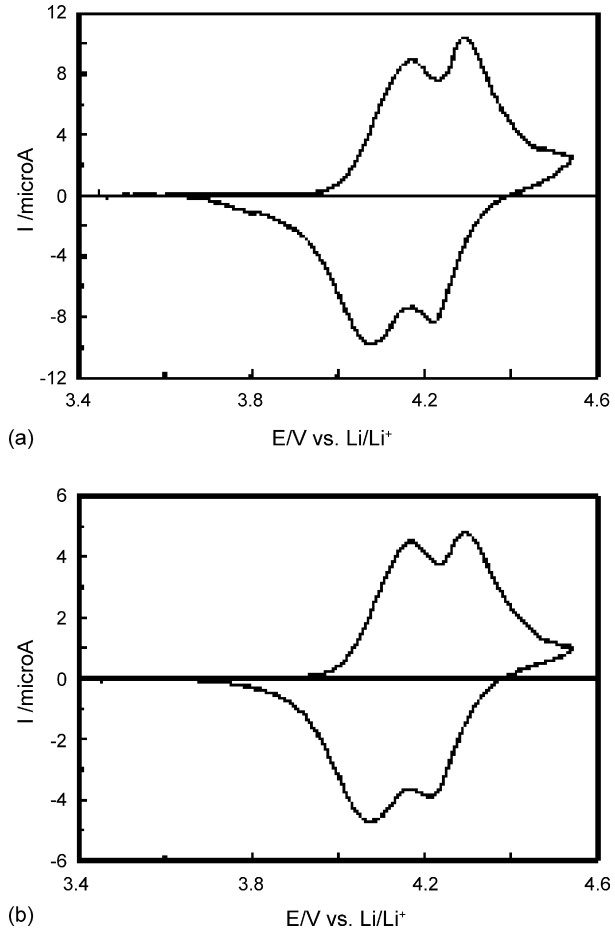

Fig. 8. Cyclic voltammograms of the $LiW_{0.01}Mn_{1.99}O_4$ samples prepared from (a) metallic W powder, and (b) WO_3 under quasi-steady state condition. Scan rate 0.1 mV/s.

W just occurs in situ across the spinel structure to form strong W–O bonds, there is a better dopant distribution and formation of appropriate W–O bonds leads to more stable spinel structure. Cycleability of cathode materials depends on various parameters such morphology, since it is known that cathode surface is

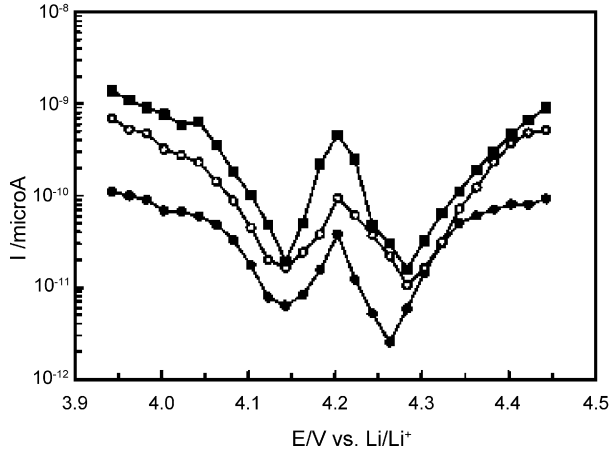

Fig. 9. Plots of diffusion coefficient versus potential for $LiMn_2O_4$ (●),$LiW_{0.01}Mn_{1.99}O_4$ prepared from metallic W powder (■), $LiW_{0.01}Mn_{1.99}O_4$ prepared from WO_3 (◯).

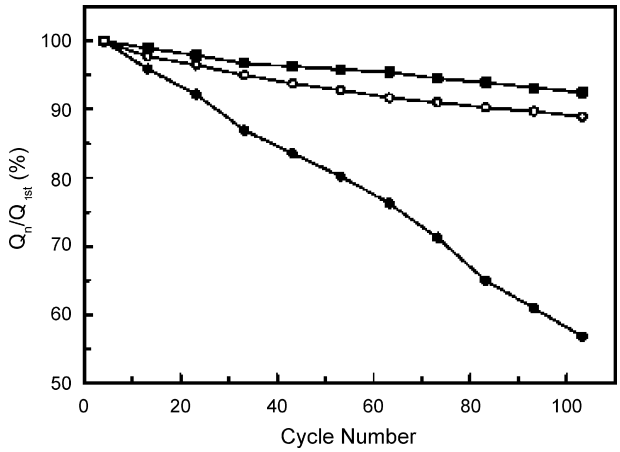

Fig. 10. Cycleabilities of the $LiW_{0.01}Mn_{1.99}O_4$ samples prepared from metallic W powder (◯), and WO_3 (■), as detected from cyclic voltammetric measurements with scan rate of 0.1 mV/s. Cycleability of the virgin $LiMn_2O_4$ cathode material (●) was also presented for comparison.

subject of severe structural changes [37]. It is well known that particle size strongly affects battery performance of $LiMn_2O_4$ cathode [38,39]. This may provide different pathways for lithium diffusion [40]. Even, metal oxide particles incorporated within $LiMn_2O_4$ particles (not into the $LiMn_2O_4$ lattice) may provide appropriate paths for Li diffusion, leading to better battery performance [41,42]. On the other hand, incorporation of dopant may significantly affect the morphology of $LiMn_2O_4$ spinel [43], as it was also detected for the case of W incorporation. However, these are just speculations, and further experimental evidences from extensive investigations are needed to understand this difference. Nevertheless, the results are completely satisfactory from applied point of view, as it introduces a simple approach for improvement of $LiMn_2O_4$ cathode. As the final words, it should be emphasized that the aim of the present paper is not to make an exact conclusion about this typical case. Instead, we wish to attract the attention of researchers studying lithium batteries to such features from a different aspect. Cyclic voltammetry can offer a visual thinking about the phenomena occurring for similar cases in such comparative study, though charge/discharge profiles also confirmed the conclusions made here via a quantitative analysis.

4. Conclusion

Extensive investigation of W substitution for improvement of battery performance of $LiMn_2O_4$ spinel was performed. In this preliminary stage, the effects of W substitution from different raw materials on spinel structure, powder morphology, and electrochemical performances of the cathode material were investigated before deep investigations of battery performance by means of conventional battery tests. It is obvious that tungsten is an appropriate transition metal for metal substitution in $LiMn_2O_4$ to improve its battery performance. According to the experimental results obtained for different W concentrations, it can be concluded that the best case is $LiW_{0.01}Mn_{1.99}O_4$. On the other hand, it was found that the tungsten raw material also has a significant influence on the material properties, and each

source leads to specified improvements. Therefore, it is very important to choose an appropriate source in accordance with the desire application. Since the amount of W substituted in $LiMn_2O_4$ spinel is very small, this approach is of practical interest. Further investigations of battery performance of this novel cathode material ($LiW_{0.01}Mn_{1.99}O_4$ synthesized from metallic W powder) will reveal its advantages for practical applications.

References

[1] D. Zhang, B.N. Popov, R.E. White, J. Power Sources 76 (1998) 81.
[2] G.G. Amatucci, N. Pereira, T. Zheng, I. Plitz, J.M. Tarascon, J. Power Sources 81–82 (1999) 39.
[3] M.C. Tucker, L. Kroeck, J.A. Reimer, E.J. Cairns, J. Electrochem. Soc. 149 (2002) A1409.
[4] M.C. Tucker, J.A. Reimer, E.J. Cairns, J. Electrochem. Soc. 149 (2002) A574.
[5] J.-S. Kim, J.T. Vaughy, C.S. Johnson, M.M. Thackeray, J. Electrochem. Soc. 150 (2003) A1498.
[6] Y.W. Tsai, R. Santhanam, B.J. Hwang, S.K. Hu, H.S. Sheu, J. Power Sources 119–121 (2003) 701.
[7] Y. Shin, A. Manthiram, J. Electrochem. Soc. 151 (2004) A204.
[8] Y. Ein-Eli, W.F. Howard, S.H. Lu, S. Mukerjee, J. McBeen, J.T. Vaughey, M.M. Thackeray, J. Electrochem. Soc. 145 (1998) 1238.
[9] Q. Zhang, A. Banakdarpour, M. Zhang, Y. Gao, J.R. Dahn, J. Electrochem. Soc. 144 (1997) 205.
[10] H. Kawai, M. Nagata, H. Tukamoto, A.R. West, J. Power Sources 81–82 (1999) 67.
[11] Y. Idemoto, H. Narai, N. Koura, J. Power Sources 119–121 (2003) 125.
[12] R. Alcantara, M. Jaraba, P. Lavela, J.L. Tirado, Ph. Biensan, A. de Guibert, C. Jordy, J.P. Peres, Chem. Mater. 15 (2003) 2376.
[13] G.T.-K. Fey, C.-Z. Lu, T.P. Kumar, J. Power Sources 115 (2003) 332.
[14] A. Eftekhari, J. Power Sources 132 (2004) 240.
[15] A. Eftekhari, J. Power Sources 124 (2003) 182.
[16] R. Chitrakar, H. Kanoh, Y. Makita, Y. Miyai, K. Ooi, J. Mater. Chem. 10 (2000) 2325.
[17] A. Eftekhari, Electrochim. Acta 47 (2001) 495.
[18] A. Eftekhari, A. Bayandori Moghaddam, M. Solati-Hashjin, J. Alloy. Compd. 424 (2006) 225–230.
[19] D.D. MacNeil, J.R. Dahn, J. Electrochem. Soc. 150 (2003) A21.
[20] Y. Hu, W. Kong, Z. Wang, X. Huang, L. Chen, Solid State Ionics 176 (2005) 53.
[21] A. Eftekhari, J. Electrochem. Soc. 151 (2004) A1456.
[22] M. Jayalakshmi, M. Mohan Rao, F. Scholz, Langmuir 19 (2003) 8403.
[23] J.-W. Lee, S.-I. Pyun, Electrochim. Acta 49 (2004) 753.
[24] N. Li, C.J. Patrissi, G. Che, C.R. Martin, J. Electrochem. Soc. 147 (2000) 2044.
[25] J. Kohler, H. Makihara, H. Uegaito, H. Inoue, M. Toki, Electrochim. Acta 46 (2000) 59.
[26] S.S. Zhang, T.R. Jow, J. Power Sources 109 (2002) 172.
[27] J.-H. Kim, S.-T. Myung, C.S. Yoon, I.-H. Oh, Y.-K. Sun, J. Electrochem. Soc. 151 (2004) A1911.
[28] Y. Sun, C. Quyang, Z. Wang, X. Huang, L. Chen, J. Electrochem. Soc. 151 (2004) A504.
[29] B. Deng, H. Nakamura, M. Yoshio, J. Power Sources 141 (2005) 116.
[30] K. Asakura, S. Okada, H. Arai, S.-i. Tobishima, Y. Sakurai, J. Power Sources 81–82 (1999) 388.
[31] H. Tang, C.Q. Feng, Q. Fan, T.M. Lei, J.T. Sun, L.J. Yuan, K.L. Zhang, Chem. Lett. (2002) 822.
[32] A. Eftekhari, Electrochim. Acta 50 (2005) 2541.
[33] J. Barker, K. West, Y. Saidi, R. Pynenburg, B. Zachau-Christiansen, R. Koksbang, J. Power Sources 54 (1995) 475.
[34] A. Eftekhari, J. Electrochem. Soc. 151 (2004) A1816.
[35] H.-T. Chung, S.-T. Myung, T.-H. Cho, J.-T. Son, J. Power Sources 97–98 (2001) 454.
[36] Y.-K. Sun, C.S. Yoon, C.K. Kim, S.G. Youn, Y.-S. Lee, M. Yoshio, I.-H. Oh, J. Mater. Chem. 11 (2001) 2519.
[37] A. Eftekhari, Electrochim. Acta 48 (2003) 2831.
[38] R. Vacassy, H. Hofmann, N. Papageorgiou, M. Gratzel, J. Power Sources 81–82 (1999) 621.
[39] C.-H. Lu, S.-W. Lin, J. Power Sources 97–98 (2001) 458.
[40] A. Eftekhari, Solid State Ionics 161 (2003) 41.
[41] A. Eftekhari, J. Electrochem. Soc. 150 (2003) A966.
[42] A. Eftekhari, Solid State Ionics 167 (2004) 237.
[43] A. Eftekhari, F. Moztarzadeh, M. Kazemzad, J. Phys. D: Appl. Phys. 38 (2005) 628.